IMMUNOLOGY

10.1126/sciadv.1500637

Neuron-specific SALM5 limits inflammation in the CNS via its interaction with HVEM

Yuwen Zhu,[1]* Sheng Yao,[1]* Mathew M. Augustine,[2] Haiying Xu,[2] Jun Wang,[1] Jingwei Sun,[1] Megan Broadwater,[2] William Ruff,[2] Liqun Luo,[1] Gefeng Zhu,[1] Koji Tamada,[2] Lieping Chen[1,2†]

The central nervous system (CNS) is an immune-privileged organ with the capacity to prevent excessive inflammation. Aside from the blood-brain barrier, active immunosuppressive mechanisms remain largely unknown. We report that a neuron-specific molecule, synaptic adhesion-like molecule 5 (SALM5), is a crucial contributor to CNS immune privilege. We found that SALM5 suppressed lipopolysaccharide-induced inflammatory responses in the CNS and that a SALM-specific monoclonal antibody promoted inflammation in the CNS, and thereby aggravated clinical symptoms of mouse experimental autoimmune encephalomyelitis. In addition, we identified herpes virus entry mediator as a functional receptor that mediates SALM5's suppressive function. Our findings reveal a molecular link between the neuronal system and the immune system, and provide potential therapeutic targets for the control of CNS diseases.

INTRODUCTION

The immune-privilege status of the central nervous system (CNS) was considered exclusively as a function of the blood-brain barrier (BBB), a unique structure largely consisting of endothelial cells and astrocytic end feet surrounding all capillaries within the CNS. More recently, this traditional view has been challenged by experimental findings that peripheral immune cells can cross the intact BBB and enter the CNS (*1*). Supporting that, a recent study discovered that the brain is directly connected to the immune system by lymphatic vessels (*2*). In addition, residential neuronal and microglial cells within the CNS can actively down-regulate ongoing inflammatory immune responses (*3*–*5*). Neurons can also execute their immunoregulatory role through direct contact with T cells (*6*, *7*). A growing body of evidence reveals that certain infiltrating immune cells can be neuroprotective even during neuroinflammation (*8*–*10*). Therefore, the CNS appears to have a unique microenvironment that actively contains the spread of inflammatory immune responses, thereby maintaining tissue integrity of the organ.

The presence of active immunosuppressive mechanisms contributes tremendously to the establishment and maintenance of immune privilege in the CNS. One such molecular mechanism that is known to protect neurons from attack by natural killer (NK) cells is the induced expression of human leukocyte antigen (HLA)–G receptors that bind NK inhibitory receptors, such as NK cell immunoglobulin (Ig)–like receptors (*11*). Astrocytes also play a role by up-regulating surface molecules such as FasL and B7-H1 (PD-L1), which promote activated T cell apoptosis by engaging Fas and PD-1 receptors, respectively (*12*, *13*). In addition, microglial cells can inhibit T cell proliferation by mediating depletion of tryptophan via IDO (indoleamine 2,3-dioxygenase) (*14*). Neurons can suppress the activation of microglial cells/macrophages through several cell surface receptor–ligand interactions, including CD47/SIRPα (signal regulatory protein α), CD200/CD200L, and fractalkine/CX3CR1 (*15*). Furthermore, both neurons and astrocytes secrete transforming growth factor–β (TGF-β), a powerful suppressor that prevents the activation of T cells, NK cells, and macrophages (*16*, *17*).

Here, we identify SALM5 (synaptic adhesion-like molecule 5) as a potential contributor to immune privilege in the CNS. We show that administration of a SALM5 monoclonal antibody (mAb) exacerbates inflammation in the CNS. Finally, we also identified herpes virus entry mediator (HVEM) (also known as TNFRSF14), a member of the tumor necrosis factor receptor (TNFR) superfamily, as the responsible counter-receptor for SALM5.

RESULTS

SALM5 is a candidate associated with immune privilege

We used a bioinformatics approach to search for molecules that are selectively expressed in immune-privileged tissues and organs. Genes with elevated expression in the brain (1134), placenta (294), and testis (1925) were identified using the Human Protein Atlas. Because the Ig superfamily (IgSF) is one of the largest families actively involved in immunomodulation, we selected 37 Ig-containing surface molecules from these genes for further analysis (Fig. 1A). We manually examined the expression profiles of these 37 genes in several gene expression databases, including BioGPS, the Immunological Genome Project (ImmGen), and the Human Proteome Map (HPM). Then, we finally focused on 15 genes with selective expression in human immune-privileged organs (fig. S1). One noticeable observation is that 5 of these 15 genes belong to the *SALM* gene family (Fig. 1B). SALMs, also known as LRFNs (leucine-rich and fibronectin III domain–containing proteins), are a group of newly characterized adhesion molecules predominantly expressed in the CNS. The five members of the SALM family are type I transmembrane proteins, with a typical extracellular structure composed of leucine-rich repeats (LRRs), an Ig-like domain, and a fibronectin type III (FN) domain. Members of the SALM family are known for their involvement in neurite outgrowth and synapse formation (*18*–*20*).

Ultimately, we selected SALM5 for further study because recombinant SALM5-Ig fusion protein showed clear staining with several types of immune cells, including $CD4^+$ T cells, $CD8^+$ T cells, and B cells

[1]Department of Immunobiology, Yale School of Medicine, New Haven, CT 06520, USA. [2]Department of Oncology, Johns Hopkins University School of Medicine, Baltimore, MD 21231, USA.
*These authors contributed equally to this work.
†Corresponding author. E-mail: lieping.chen@yale.edu

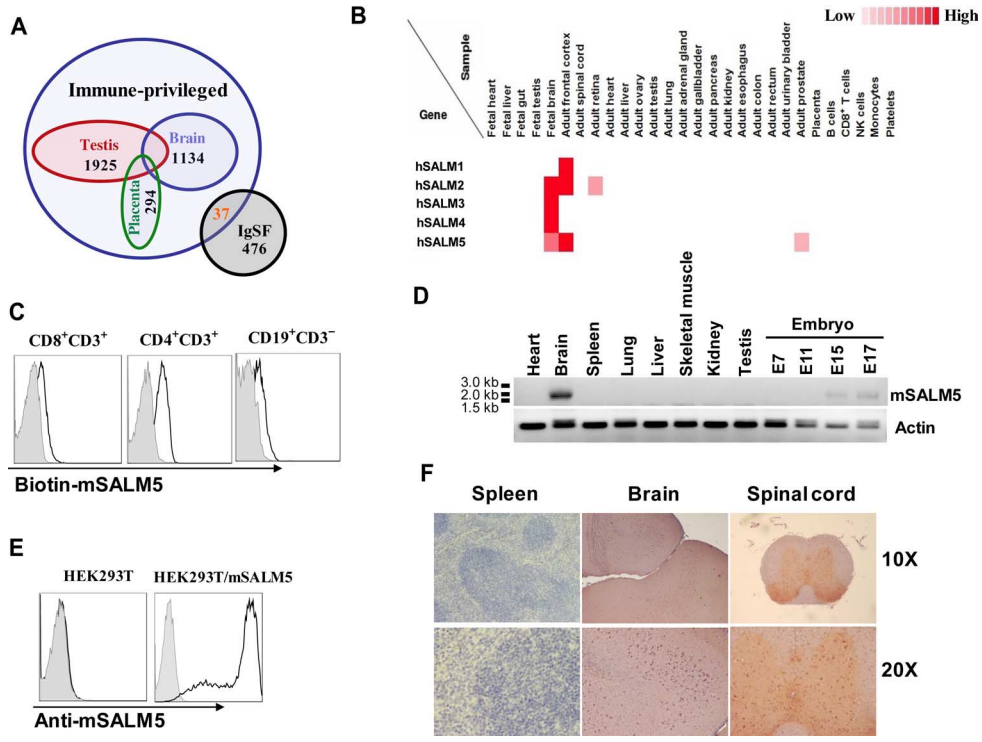

Fig. 1. Identifying *SALM5* as a gene specifically expressed in the CNS. (**A**) Strategy used to identify molecules with Ig-like domains that are enriched in immune-privileged organs. (**B**) Expression profile of the SALM family in different human organs or cell types. (**C**) Staining of lymphocytes (as indicated from normal mice) for SALM5 fusion protein binding by flow cytometry. (**D**) SALM5 mRNA expression in different mouse tissues determined by reverse transcription polymerase chain reaction (RT-PCR). (**E**) SALM5 mAb (clone 7A10) staining of human embryonic kidney 293T (HEK293T) cells transfected with mouse SALM5 (mSALM5) full-length (right panel) or control (left panel) plasmid. (**F**) Expression of SALM5 in normal tissues. Paraffin-embedded naïve mouse tissues (as indicated) were stained using a biotin-labeled SALM5 mAb.

(Fig. 1C). This result implied the presence of a putative counter-receptor for SALM5 on these cells, and the SALM5-mediated interaction might be involved in regulating immune responses within immune-privileged tissues. As shown in Fig. 1D, SALM5 mRNA was only detected in the brain, but not in other organs, including the heart, spleen, lung, liver, and skeletal muscle. We then generated a SALM5 mAb (clone 7A10) by immunization of a hamster, and demonstrated that this mAb is highly specific to both mouse and human SALM5 (Fig. 1E). Immunohistochemical analysis of mouse tissues with 7A10 demonstrated that SALM5 protein is constitutively expressed in the brain and spinal cord, but not in the spleen (Fig. 1F); the staining pattern was similar to two commercially available SALM5 antibodies (fig. S2). In addition, Western blot analysis of mouse tissues further demonstrated that SALM5 is restrictively expressed in the brain (fig. S3). Our results thus indicate that SALM5 is constitutively and selectively expressed in the CNS.

SALM5 inhibits microglia/ macrophage-mediated neuroinflammation

To determine whether SALM5 is indeed involved in CNS inflammation, we administered lipopolysaccharide (LPS) systemically, which induces CNS inflammation by activating microglial cells (*21*). In this model, SALM5 mAb treatment significantly increased microglial cell activation in the spinal cord, as evidenced by the intensified staining of ionized calcium binding adaptor molecule 1 (Iba-1), a marker specific for activated macrophages and/or microglia (Fig. 2A). The treatment by SALM5 mAb did not affect LPS-triggered inflammation systemically, as revealed by insignificant changes in inflammatory cytokines in the serum in comparison with the control (fig. S4). This is consistent with the CNS-restricted expression profile for SALM5. SALM5 fusion protein bound directly to microglia cells isolated from wild-type mice, and the SALM5 mAb effectively blocked this interaction (Fig. 2B), suggesting that the effect of our SALM5 mAb might be to disrupt a suppressive effect of SALM5 on microglia cells. To test whether SALM5 directly suppresses microglia/macrophage activation, we used a cell culture system in which macrophages were isolated from the peritoneal cavity and were preincubated with SALM5- or mock-transfected HEK293T cells for 12 hours before LPS activation. Proinflammatory cytokines interleukin-6 (IL-6) and TNFα were measured in cultured supernatants using a specific sandwich enzyme-linked immunosorbent assay (ELISA). As shown in Fig. 2C, the production of both IL-6 and TNFα from the cultured macrophages was significantly inhibited by $SALM5^+$ HEK293T cells. Therefore, SALM5 directly suppressed macrophage activation, likely by engaging a putative receptor on macrophages.

HVEM is the counter-receptor for SALM5

To identify the counter-receptor for SALM5, we screened a receptor-ligand proteome with a human SALM5-Ig fusion protein (*22*, *23*). In addition to the wells containing FcR and OCLN (occludin) as internal positive controls, we found one positive hit for SALM5 binding, which we determined was HVEM (Fig. 3A and fig. S5A). The specificity of this interaction was further verified by flow cytometry (Fig. 3B). mSALM5

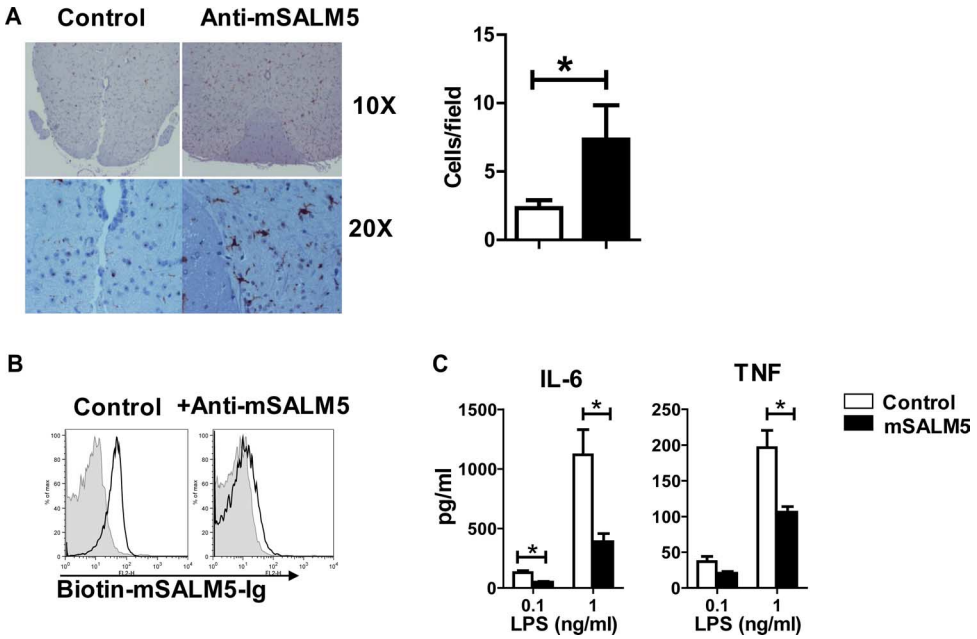

Fig. 2. SALM5 mAb treatment enhanced inflammation in the CNS. (**A**) Mice treated with SALM5 mAb or control antibody were intravenously injected with LPS. Twenty-four hours later, mice were sacrificed and their spinal cords were stained to detect the expression of Iba-1. Data are representative of three experiments with three mice in each group. (**B**) Isolated microglia from naïve B6 mice were stained using biotin-conjugated mSALM-Ig, which was preincubated with control or anti-SALM5 mAb. (**C**) Peritoneal macrophages were isolated and cultured overnight with irradiated SALM5^{+} HEK293T cells or control HEK293T cells. LPS was added to the culture at the indicated doses for 8 hours. The culture medium was then harvested and tested for cytokines. Data are representative of two independent experiments. *$P < 0.05$ (unpaired Student's t test).

fusion protein bound strongly to HEK293T cells transfected with mHVEM, but not to control cells, and inclusion of an HVEM mAb completely blocked this interaction. Using hHVEM-Ig fusion protein to screen the library, we further validated the specificity of this interaction between SALM5 and HVEM. Besides LIGHT, B and T lymphocyte attenuator (BTLA), and CD160, which are all known counter-receptors for HVEM (*24*–*26*), the only other well that contained a strong positive signal was the well containing human SALM5 (Fig. 3C and fig. S5B). The HVEM-Ig screening did not generate any positive signal in the wells containing the other four SALM family members, though members of the SALM family share about 50% homology in their protein sequences. These interactions were further validated in both humans and mice by flow cytometry (Fig. 3, D and E). Inclusion of the SALM5 mAb 7A10 completely blocked the binding of mHVEM-Ig to mSALM5-transfected cells (Fig. 3F), indicating that this SALM5 mAb is a blocking antibody for the SALM5-HVEM interaction.

SALM5 interacts with the HVEM CRD1 region through its LRR domain

The HVEM molecule uses four cysteine-rich domains (CRDs) to interact with its counter-receptors (*27*, *28*). Both BTLA and CD160 belong to the IgSF and have been shown to bind the HVEM CRD1 region, whereas LIGHT, a TNF superfamily member, binds the CRD2 and CRD3 regions without interfering with BTLA or CD160 binding (*29*). To dissect the interactions of SALM5 with other HVEM counter-receptors, we first preincubated an HVEM transfectant with BTLA, CD160, or LIGHT fusion protein and subsequently stained cells with biotin-labeled SALM5 protein. The addition of BTLA or CD160 protein completely blocked the binding of SALM5 to the HVEM transfectant, whereas preinclusion with LIGHT protein had a marginal effect on SALM5 binding (Fig. 4A). Our data indicate that SALM5 binds HVEM via the CRD1 domain. To further confirm this interaction, we used site-directed mutagenesis to construct an HVEM deletion mutant that lacked the CRD1 domain (ΔHVEM), and a series of HVEM point mutations within the CRD1 region, which have proven to be important for the BTLA-HVEM interaction (*30*, *31*). HEK293T cells were transfected with plasmids harboring wild-type HVEM, ΔHVEM without CRD1, and CRD1 mutations. Polyclonal HVEM antibody staining confirmed similar levels of HVEM surface expression (Fig. 4B, upper panel). Deleting the CDR1 region of HVEM completely eliminates SALM5 binding, demonstrating that the CDR1 domain of HVEM is essential for the HVEM-SALM5 interaction. In addition, Y61A and V74A point mutations largely lost their ability to bind SALM5, whereas a K64A mutant only had a marginal effect on the SALM5-HVEM interaction (Fig. 4B, lower panel). Meanwhile, this same K64A mutation significantly affected the CD160-HVEM interaction but minimally affected the BTLA-HVEM interaction (fig. S6). Together, these data demonstrate that SALM5 interacts with the CRD1 domain on HVEM via an overlapping binding site for both BTLA and CD160.

The extracellular domain of SALM5 contains an LRR domain, an Ig-like domain, and an FN domain. To identify the binding domain within the SALM5-HVEM interaction, we generated a series of SALM5 chimeras for analysis by replacing each SALM5 domain with a corresponding portion from SALM3 (Fig. 4C). As expected, HVEM interacted with the HEK293T/SALM5-transfected cells, but not the SALM3 transfectant. The LRR domain, but not the Ig or FN domain from SALM5, is sufficient to endow the binding capacity to HVEM (Fig. 4D). Consistently,

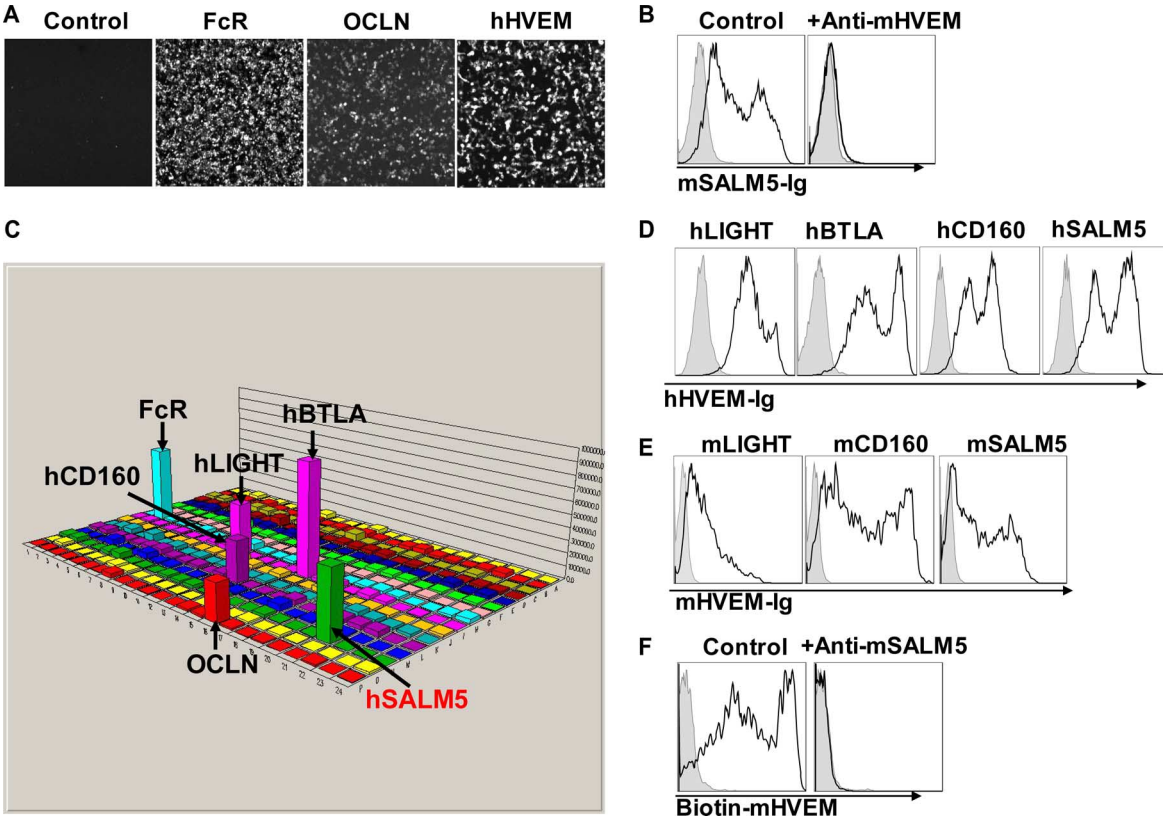

Fig. 3. Identification of HVEM as the counter-receptor for SALM5. (**A**) A library of human transmembrane genes was screened using purified recombinant SALM5 fusion protein. Graphic views of individual wells with positive hits for SALM5-Ig are shown. (**B**) HEK293T cells transfected with mouse HVEM (mHVEM) were stained by mSALM5-Ig in the presence of control mAbs (left panel) or HVEM mAb (right panel). (**C**) HVEM counter-receptors were screened by CDS. A three-dimensional illustration of the results from one 384-well plate is shown; all positive hits for HVEM-Ig are indicated. (**D**) Human HVEM (hHVEM) interacted with four counter-receptors. HEK293T cells were transiently transfected to express human genes, as indicated, and were stained with hHVEM-Ig (open histograms) or control Ig (filled histograms). (**E**) mHVEM interacted with mouse counter-receptors. HEK293T cells were transiently transfected to express mLIGHT, mCD160, or mSALM5, and were stained with mHVEM-Ig (open histograms) or control Ig (filled histograms). (**F**) Anti-SALM5 mAb (clone 7A10) blocked the SALM5-HVEM interaction. HEK293T cells were transiently transfected with the plasmid encoding mSALM5 (open) or the control plasmid (close). HEK293T transfectants were preincubated with control antibody or anti-SALM5 mAb before being stained with mHVEM-Ig.

our SALM5-blocking mAb (clone 7A10) bound to the LRR domain of SALM5 (fig. S7). This interaction revealed another type of domain structure that HVEM can bind. To our knowledge, this is the first molecular evidence that a TNFR member binds an LRR domain structure.

Blocking the SALM5-HVEM interaction using SALM5 mAb aggravates experimental autoimmune encephalomyelitis

Finally, we tested the effect of this SALM5-blocking mAb in mouse experimental autoimmune encephalomyelitis (EAE), an animal model of CNS inflammation. We treated wild-type and HVEM$^{-/-}$ mice with SALM5 mAb or control antibody 10 days after MOG (myelin oligodendrocyte glycoprotein) immunization, when mice start to show clinical symptoms. Notably, EAE was relatively more severe in HVEM$^{-/-}$ mice in comparison with wild-type mice (Fig. 5A), which is consistent with a previous report (*32*). The SALM5 mAb was not effective in HVEM$^{-/-}$ mice, whereas the identical treatment of wild-type mice with this mAb aggravated EAE in terms of both disease onset and peak severity (Fig. 5A). About 30% of the mice treated with SALM5 mAb died, whereas all of the mice treated with the control antibody survived. We thus conclude that the effect of SALM5 mAb on EAE is dependent on endogenous HVEM, and the role of this mAb in vivo is to block the SALM5-HVEM interaction.

We further analyzed spinal cord sections from wild-type mice treated with control or SALM5 mAb by hematoxylin and eosin (H&E), and immunohistochemical staining. Mice treated with SALM5 mAb developed extensive inflammation that was characterized by a massive infiltration of mononuclear cells (Fig. 5B, arrows). Immunohistochemical staining determined that these inflammatory cells in the spinal cord were predominantly CD3$^+$ T cells and MAC3$^+$ macrophages (Fig. 5B). Mononuclear cells were isolated from the CNS of EAE mice and were analyzed by flow cytometry. There were approximately four times as many infiltrating CD45$^+$ cells in mice that were treated with SALM5 mAb compared with control mice (Fig. 5C). Of those CD45$^+$ cells, the increase in CD4$^+$ T cells and CD11b$^+$CD45^{hi} macrophages accounted for most of the total increase in cell number observed in the SALM5 mAb–treated mice, which was consistent with the observed immunohistochemical staining (Fig. 5D).

RT-PCR analysis of diseased CNS tissues revealed up-regulation of the proinflammatory cytokines IL-6 and TNF after SALM5 mAb treatment (Fig. 5E). Immunohistochemistry of the SALM5 mAb–treated

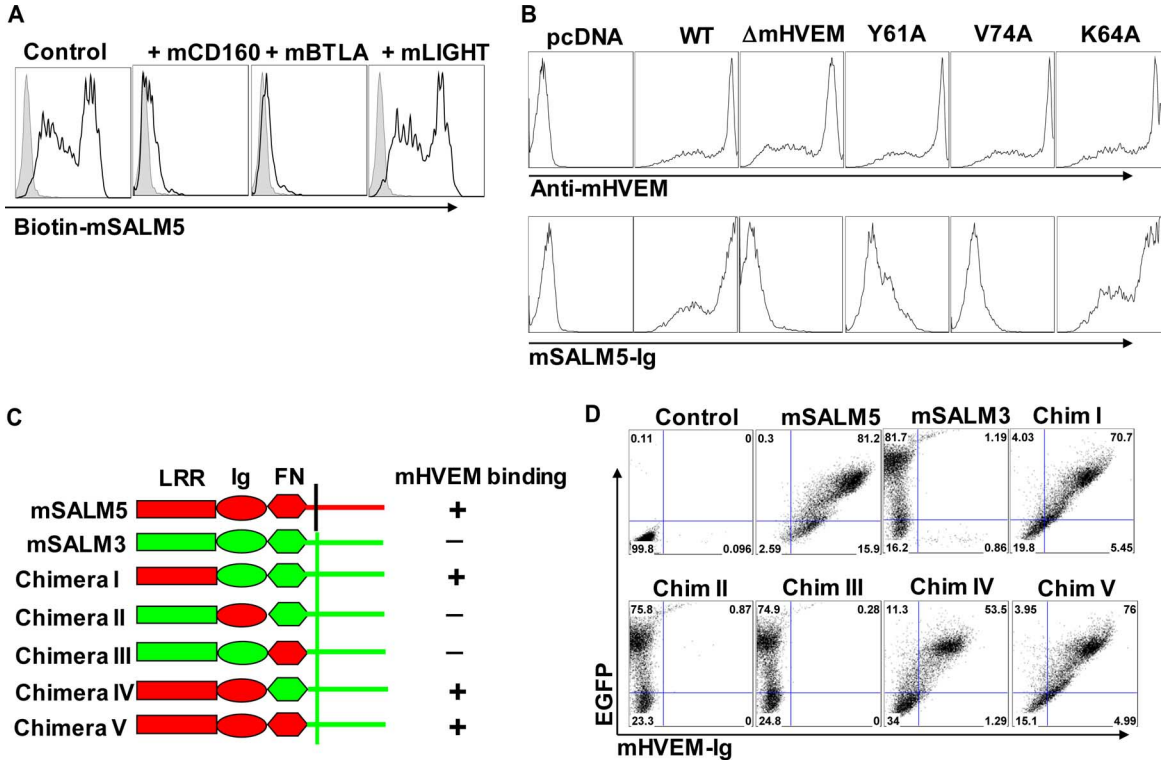

Fig. 4. Binding sites in the SALM5-HVEM interaction. (**A**) Competitive binding of SALM5 with other HVEM counter-receptors. HEK293T cells transfected with mHVEM were incubated with mBTLA, mCD160, or mLIGHT recombinant fusion proteins before being stained by biotin-labeled mSALM5-Ig. (**B**) Identification of the interacting domain on HVEM. Full-length HVEM [wild-type (WT)], HVEM without the CRD1 domain, or HVEM mutants with point mutation, as indicated, were individually expressed in HEK293T cells and stained with SALM5-Ig (lower panels). The expression of WT and mutated HVEM was verified by HVEM polyclonal antibody staining (upper panels). (**C** and **D**) Identification of the binding domain on SALM5 for HVEM. Each extracellular domain for SALM5, including LRR, Ig, and FN, was swapped with the corresponding domain on SALM3 using PCR cloning and fused to a C-terminal enhanced green fluorescent protein (EGFP). These chimeric mutants were transiently expressed in HEK293T cells and stained using mHVEM-Ig. A summary of the binding assay by flow cytometry (D), positive binding to mHVEM (+), or negative binding to mHVEM (–) was indicated (C).

CNS sections from mice showed an increased expression of Iba-1 (Fig. 5F) (*33*, *34*). Consistent with these results, microglial cells from CNS in SALM5 mAb–treated mice expressed higher levels of major histocompatibility complex (MHC) class II and CD80 (Fig. 5G), which may explain the increased numbers of $CD4^+$ T cells in the CNS seen in SALM5 mAb–treated mice. We also examined the ability of freshly isolated CNS microglia/macrophages to produce proinflammatory cytokines upon SALM5 mAb treatment ex vivo. Microglia/macrophages were purified from SALM5 mAb– or control mAb–treated mice and cultured for 12 hours without any stimulation; the cultured supernatants were measured using sandwich ELISA. The cultures from SALM5 mAb–treated mice produced significantly higher levels of proinflammatory cytokines, including IL-6, TNF-α, and IL-10, than those from control mAb (Fig. 5H). Collectively, our results support an important role for SALM5 mAb in the activation of microglia/macrophages in the CNS and implicate a suppressive role for SALM5-expressing neuronal cells in microglia/macrophage-mediated neuroinflammation.

Although HVEM is expressed in T cells and accumulated T cells were found in the CNS of SALM5 mAb–treated mice with EAE, our studies suggest that SALM5 does not directly regulate T cell functions in EAE. First, coated SALM5 did not costimulate T cells in the presence of CD3 mAb (fig. S8A). Second, the expression of membrane-bound SALM5 on the K^b-OVA transfectant had no effect on OT-I T cell proliferation, as measured by the dilution of carboxyfluorescein diacetate succinimidyl ester (fig. S8B). Finally, in an adoptive transfer EAE model where purified HVEM-deficient 2D2 transgenic T cells were transferred to induce disease, the treatment of SALM5 mAb still exacerbated EAE (fig. S8C). Together, we conclude that SALM5 interacts with HVEM to limit inflammation in the CNS and therefore indirectly affects CNS T cell infiltration in EAE.

DISCUSSION

Here, we identify and characterize an organ-specific pathway, which modulates inflammatory immune responses in the CNS. In this pathway, SALM5, a molecule mainly found in neuronal cells, interacts with HVEM in myeloid cells to suppress neuroinflammation in the CNS. Our findings uncover the molecular mechanism for this negative regulation and control of neuroinflammation, and also provide an explanation for the long-standing puzzle and the source of immune privilege in the CNS. Our findings provide potential therapeutic targets for the treatment of inflammatory neurological diseases.

Our competitive binding and mutagenesis studies revealed several important features of the interaction between SALM5 and HVEM. First, the SALM5-HVEM interaction is highly specific and is species-conserved. The SALM family has five molecules that have been characterized. The

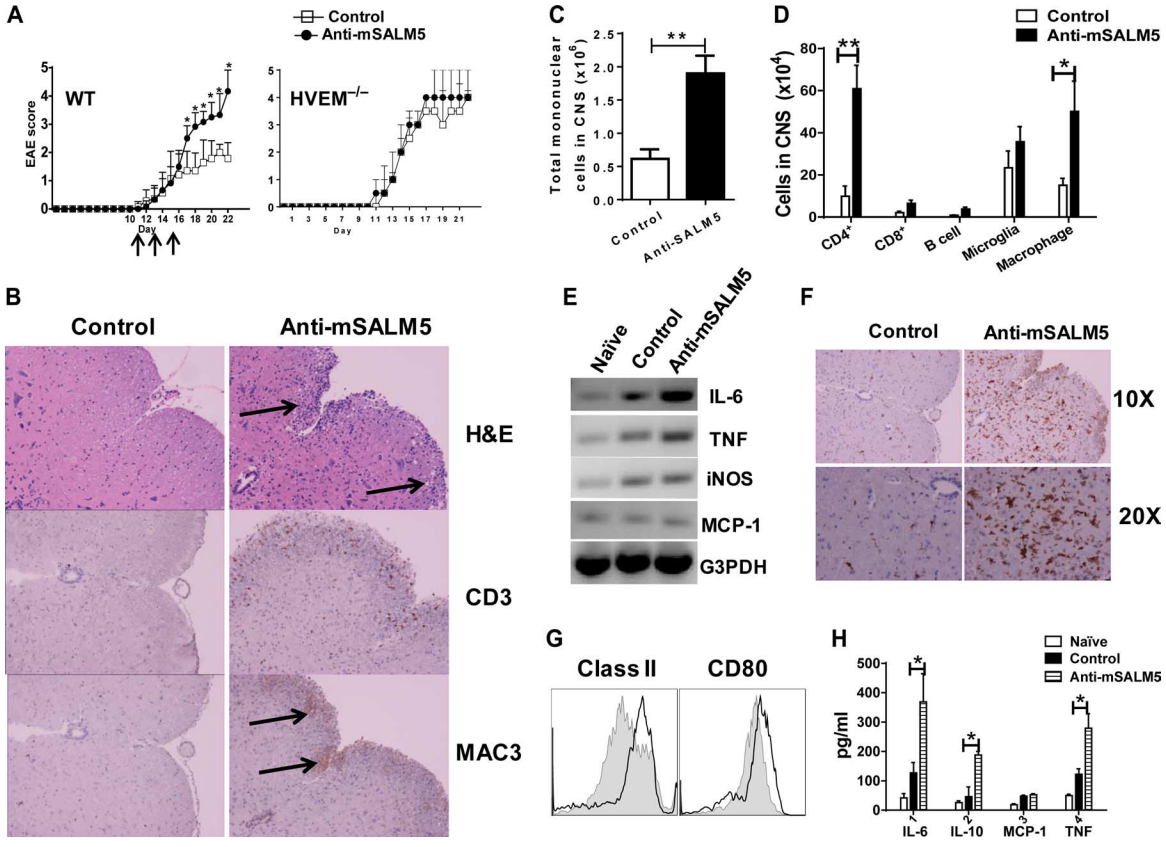

Fig. 5. SALM5 interacts with HVEM to inhibit EAE. (**A**) Aggravation of EAE induced by blocking of the SALM5-HVEM interaction. WT and HVEM-knockout mice (HVEM$^{-/-}$) were immunized with MOG(35–55) peptide to induce EAE. SALM5 mAb or control antibody was given on days 10, 14, and 17 after MOG immunization (n = 7). Clinical scores of EAE were measured daily. Representative results from three independent experiments are shown. *P < 0.05 (unpaired Student's t test). (**B**) Pathology of spinal cord sections from mice on day 19 after EAE induction. Inflammatory infiltrates in spinal cords were revealed using H&E staining. The infiltrates were further visualized by staining with mAb against CD3 for T cells or with mAb against MAC3 for macrophages. (**C** and **D**) Quantification of infiltrating mononuclear cells in the CNS. The mouse brains and spinal cords were prepared and extracted on day 19 after EAE induction. Total numbers of mononuclear cells (C), as well as the respective numbers of CD4$^+$ T cells, CD8$^+$ T cells, B cells, macrophages, and microglia (D) in the CNS were counted using flow cytometry. Data are representative of three independent experiments with five mice in each group. *P < 0.05 (unpaired Student's t test). (**E**) RT-PCR detection of the proinflammatory cytokine mRNA levels in the spinal cords of naïve mice or mice treated with SALM5 mAb or control antibody after EAE induction. (**F**) Immunohistochemical staining of activated microglia by Iba-1 expression in the spinal cords of mice with EAE. The folds of amplification in the micrograph are shown on the right. (**G**) Expression of MHC class II and CD80 in microglia cells isolated from the CNS after EAE induction with SALM5 mAb (open histogram) or control antibody (shaded histogram) treatment. Data are representative of two independent experiments with three mice in each group. (**H**) Levels of proinflammatory cytokines secreted by microglia/macrophages. The microglia/macrophages were isolated from the CNS of naïve, control antibody, or anti-SALM5 mAb–treated mice 16 days after immunization. Cells were cultured without further stimulation, and the supernatants were harvested after 12 hours. Different cytokine levels were measured using the BD Cytometric Bead Array (CBA) mouse inflammatory cytokine kit. Data are representative of three independent experiments with three mice in each group. *P < 0.05 (unpaired Student's t test).

sibling SALM family members, though sharing ~50% protein sequence identity with SALM5, do not bind HVEM, indicating a specific interaction. The second important feature is that SALM5 interacts with a "suppressive domain" on HVEM. HVEM interacts with multiple molecules to execute various immunomodulatory functions, from lymphocyte costimulation to T cell suppression. The functional diversity of this molecule relies on the interactions between its different domains and its distinct ligands. The CRD1 domain interacts with BTLA and CD160 to inhibit T cell responses (*25*, *26*), though the directionality of the signaling underlying these interactions has yet to be elucidated. On the other hand, the CDR2/3 domains of HVEM bind LIGHT and LTα, and transmit a costimulatory signal to T cells (*35*, *36*). Our studies unambiguously demonstrate that SALM5 interacts with the CRD1 domain of HVEM and competes with the binding of BTLA and CD160, but does not interfere with the LIGHT interaction. Because SALM5, BTLA, and CD160 all have inhibitory functions, HVEM's CRD1 domain appears to be exclusively suppressive. The third feature is the unique HVEM binding domain within the SALM5 molecule. Despite competing with two Ig superfamily molecules (BTLA and CD160) for HVEM binding, SALM5 interacts with HVEM through its LRR domain rather than its IgC-like domain. To the best of our knowledge, this is the first molecular evidence that a TNFR member binds an LRR domain. It appears that HVEM has the flexibility to interact with various molecular motifs, but it remains to be seen whether this phenomenon applies to other TNFR superfamily members.

Our studies support that the role of our SALM5 antibody is to disrupt the SALM5-HVEM interaction. The SALM5 mAb binds to the LRR domain of SALM5 and blocks the SALM5-HVEM binding completely (Fig. 3F and fig. S7). The effect of this antibody on EAE was fully dependent on the presence of HVEM in vivo (Fig. 5A). Similar to the parental antibody, treatment of SALM5 $F(ab')_2$ fragment significantly aggravated EAE, further excluding its in vivo effect as a depleting antibody (fig. S9).

One surprising finding in our study is that the SALM5 mAb aggravates EAE without directly affecting T cell functions. The systemic administration of SALM5 mAb does not affect T cell activation outside the CNS (fig. S4). This finding might be explained, in part, by the lack of SALM5 expression in the peripheral lymphoid organs. However, other factors may also be involved because in vitro SALM5 engagement of naïve or activated T cells, which do constitutively express HVEM, did not affect T cell activation (fig. S8). SALM5 does not appear to affect T cell functions, but instead appears to be targeting macrophages and microglial cells. In contrast to the monomer formation of BTLA and CD160, SALM5 forms a dimer, which could endow itself a unique role in HVEM signaling (fig. S10). Constitutive expression of SALM5 in neuronal cells should allow this interaction to take place because microglial cells constitutively express HVEM (fig. S11). On the basis of the constitutive expression of SALM5 in neuronal cells and HVEM in microglial cells, our results support that the SALM5-HVEM interaction serves as a default pathway that provides the suppressive mechanism responsible for maintaining immune privilege in the CNS. However, our results do not exclude a possibly immunosuppressive effect of SALM5 signal through neuron cells. Because SALM5 is known to regulate neurite growth, it is intriguing to further evaluate the effect of SALM5 signal on neuron cells upon HVEM ligation.

In conclusion, our study identified a new organ-specific pathway, which limits inflammation and contributes to the immune privilege in the CNS. In this pathway, SALM5, a surface molecule in neuronal cells, interacts with HVEM in myeloid cells to suppress inflammation in the CNS during ongoing neuroinflammation. Our findings uncover a molecular mechanism for the negative regulation and control of neuroinflammation, and provide potential therapeutic targets for the treatment of inflammatory neurological diseases.

MATERIALS AND METHODS

Bioinformatics

Genes enriched in immune-privileged organs, including the brain, placenta, and testis, were selected using the Human Protein Atlas (www.proteinatlas.org), and we further selected genes that encode membrane-bound proteins containing Ig-like domains. The enriched expression profiles of these genes in immune-privileged organs were further verified by other gene expression databases, including BioGPS, ImmGen, and HPM. Mouse orthologs of the final gene candidates were identified via the National Center for Biotechnology Information (NCBI) database, and their bindings to immune cells from normal C57BL/6 mouse splenocytes were validated by flow cytometry.

Animals, antibodies, and recombinant proteins

Female C57BL/6 mice aged 6 to 10 weeks were purchased from the National Cancer Institute, National Institutes of Health (NIH) (Frederick, MD). The $HVEM^{-/-}$ mice with a C57BL/6 background have been previously described and were provided by W. W. Hancock (*37*). All fusion proteins were generated by fusing the extracellular domain of each molecule with either mouse or human Fc tags (*38*). Hamster mAbs against mSALM5 were generated by immunizing a hamster with mSALM5-Ig fusion protein. All antibodies for flow cytometry staining, if not specified, were purchased from BD Biosciences or eBioscience.

Receptor array technology

The detailed methods used in our high-throughput screening cellular detection system (CDS) have been reported previously (*22*). Briefly, plasmids containing more than 2300 human transmembrane genes were diluted by Opti-MEM medium and placed individually into five 384-well plates at 60 ng per well. Lipofectamine 2000 was added to each well and mixed with plasmids for 30 min. Ten thousand HEK293T cells were added subsequently to each well to perform transient transfection. Eight hours after transfection, 50 ng of human SALM5-Ig or HVEM-Ig and 50 ng of anti-human Ig or anti-mouse Ig FMAT blue secondary antibody were added into each well. The plates were read 24 hours after transfection using the Applied Biosystems 8200 Cellular Detection System and analyzed using the CDS 8200 software. Each plate had a well that contained the human Fc receptor as an internal positive control for screened fusion proteins. Because OCLN expressed on transfected HEK293T cells directly interacted with the secondary antibodies that we used for screening, it was included in each plate as an indication for a successful transfection.

Plasmids for mHVEM and mSALM5 mutants

Mouse ΔHVEM was made using a PCR method similar to what was previously described (*25*). HVEM point mutations were selected as described (*30*, *31*). HVEM and SALM5 mutants were generated via PCR.

EAE model

C57BL/6 mice aged 8 to 12 weeks were immunized subcutaneously on day 0 with 100 μg of MOG(35–55) peptide emulsified in complete Freund's adjuvant (Difco). Pertussis toxin (400 ng) (Sigma) in 200 μl of phosphate-buffered saline (PBS) was injected twice, on days 0 and 2. Each mouse was injected intraperitoneally with 200 μg of SALM5 mAb or control antibody on days 10, 14, and 17. Disease severity was scored on the following scale: 0, no disease; 1, tail paralysis; 2, paraparesis; 3, paraplegia; 4, paraplegia with forelimb weakness or paralysis; 5, moribund or dead, as previously described (*39*). In some experiments, $\sim 2 \times 10^6$ naïve 2D2-transgenic T cells from wild-type or $HVEM^{-/-}$ mice were transferred intravenously into mice 24 hours before immunization.

LPS administration

C57BL/6 mice treated with pertussis toxin on days 0 and 2 were injected with 200 μg of SALM5 mAb or control antibody intracranially on day 1. On day 5, each mouse received a single intravenous dose of LPS (0.5 mg/kg) 24 hours before being sacrificed and stained for Iba-1 by immunohistochemistry.

Isolation of CNS mononuclear cells

Sacrificed mice were perfused with cold PBS before the brains and spine cords were dissected. The tissues were homogenized and digested with collagenase D and deoxyribonuclease I at 37°C for 45 min. After centrifugation, the pellets were resuspended in 30% Percoll and carefully layered on top of a 70% Percoll solution. The Percoll gradient was centrifuged at room temperature at 1000*g* for 30 min without brake. Mononuclear cells

at the 30% and 70% Percoll interphase layers were harvested and washed with complete RPMI 1640 before FACS (fluorescence-activated cell sorting) staining or in vitro culture. Microglia/macrophages were isolated by removing nonadherent cells after 2 hours in culture at 37°C.

Histology and immunohistochemistry

Tissues were removed from naïve mice or mice with EAE and embedded in paraffin. Tissues were cut into 5-μm-thick sections and stained with H&E to reveal inflammatory infiltrates. For immunohistochemistry, deparaffinized sections were stained with anti-CD3 (AbD Serotec, clone CD3-12), anti-MAC3 (AbD Serotec, clone M3/84), and anti–Iba-1 (Wako Pure Chemical Industries) according to the manufacturer's protocols. For SALM5 staining, tissues were deparaffinized and rehydrated before Ag retrieval in citrate buffer. Tissues were then stained with different SALM5 antibodies, followed by incubation with Amplification System (K1500, DakoCytomation). After horseradish peroxidase staining, slides were visualized with 3,3′-diaminobenzidine (Sigma-Aldrich).

Statistical analysis

Student's *t* test was used for statistical analysis, and *P* values reflect comparison with the control sample. *P* values less than 0.05 were considered statistically significant. The error bars in figures represent SD.

SUPPLEMENTARY MATERIALS

Supplementary material for this article is available at http://advances.sciencemag.org/cgi/content/full/2/4/e1500637/DC1

Supplementary Materials and Methods

Fig. S1. Expression profile of 15 genes enriched in immune-privileged organs.

Fig. S2. Immunostaining of SALM5 in normal mouse brain sections by different mSALM5 antibodies.

Fig. S3. Expression of SALM5 protein in mouse tissues.

Fig. S4. Effect of SALM5 mAb on LPS-induced systemic inflammation.

Fig. S5. CDS screening of a library of transmembrane proteins.

Fig. S6. Binding of the mouse BTLA and CD160 binding by mHVEM mutants.

Fig. S7. Identification of the binding domain on mSALM5 for mSALM mAb.

Fig. S8. SALM5 did not directly affect T cell proliferation.

Fig. S9. Administration of $F(ab')_2$ of SALM5 mAb aggravates EAE.

Fig. S10. SALM5, but not CD160, inhibits microglia inflammation.

Fig. S11. HVEM is highly expressed in resting lymphocytes and microglia.

REFERENCES AND NOTES

1. M. J. Carson, J. M. Doose, B. Melchior, C. D. Schmid, C. C. Ploix, CNS immune privilege: Hiding in plain sight. *Immunol. Rev.* **213**, 48–65 (2006).
2. A. Louveau, I. Smirnov, T. J. Keyes, J. D. Eccles, S. J. Rouhani, J. D. Peske, N. C. Derecki, D. Castle, J. W. Mandell, K. S. Lee, T. H. Harris, J. Kipnis, Structural and functional features of central nervous system lymphatic vessels. *Nature* **523**, 337–341 (2015).
3. E. M. Sternberg, Neural regulation of innate immunity: A coordinated nonspecific host response to pathogens. *Nat. Rev. Immunol.* **6**, 318–328 (2006).
4. L. Tian, H. Rauvala, C. G. Gahmberg, Neuronal regulation of immune responses in the central nervous system. *Trends Immunol.* **30**, 91–99 (2009).
5. K. J. Tracey, The inflammatory reflex. *Nature* **420**, 853–859 (2002).
6. Y. Liu, I. Teige, B. Birnir, S. Issazadeh-Navikas, Neuron-mediated generation of regulatory T cells from encephalitogenic T cells suppresses EAE. *Nat. Med.* **12**, 518–525 (2006).
7. V. Siffrin, H. Radburch, R. Glumm, R. Niesner, M. Paterka, J. Herz, T. Leuenberger, S. M. Lehmann, S. Luenstedt, J. L. Rinnenthal, G. Laube, H. Luche, S. Lehnardt, H.-J. Fehling, O. Griesbeck, F. Zipp, In vivo imaging of partially reversible th17 cell-induced neuronal dysfunction in the course of encephalomyelitis. *Immunity* **33**, 424–436 (2010).
8. G. Moalem, R. Leibowitz-Amit, E. Yoles, F. Mor, I. R. Cohen, M. Schwartz, Autoimmune T cells protect neurons from secondary degeneration after central nervous system axotomy. *Nat. Med.* **5**, 49–55 (1999).
9. Y. Ziv, N. Ron, O. Butovsky, G. Landa, E. Sudai, N. Greenberg, H. Cohen, J. Kipnis, M. Schwartz, Immune cells contribute to the maintenance of neurogenesis and spatial learning abilities in adulthood. *Nat. Neurosci.* **9**, 268–275 (2006).
10. E. Hauben, U. Nevo, E. Yoles, G. Moalem, E. Agranov, F. Mor, S. Akselrod, M. Neeman, I. R. Cohen, M. Schwartz, Autoimmune T cells as potential neuroprotective therapy for spinal cord injury. *Lancet* **355**, 286–287 (2000).
11. S. Rajagopalan, E. O. Long, A human histocompatibility leukocyte antigen (HLA)-G–specific receptor expressed on all natural killer cells. *J. Exp. Med.* **189**, 1093–1100 (1999).
12. P. Saas, P. R. Walker, M. Hahne, A. L. Quiquerez, V. Schnuriger, G. Perrin, L. French, E. G. Van Meir, N. de Tribolet, J. Tschopp, P. Y. Dietrich, Fas ligand expression by astrocytoma in vivo: Maintaining immune privilege in the brain? *J. Clin. Invest.* **99**, 1173–1178 (1997).
13. M. Lipp, C. Brandt, F. Dehghani, E. Kwidzinski, I. Bechmann, PD-L1 (B7-H1) regulation in zones of axonal degeneration. *Neurosci. Lett.* **425**, 156–161 (2007).
14. E. Kwidzinski, J. Bunse, O. Aktas, D. Richter, L. Mutlu, F. Zipp, R. Nitsch, I. Bechmann, Indolamine 2,3-dioxygenase is expressed in the CNS and down-regulates autoimmune inflammation. *FASEB J.* **19**, 1347–1349 (2005).
15. K. Biber, H. Neumann, K. Inoue, H. W. G. M. Boddeke, Neuronal 'On' and 'Off' signals control microglia. *Trends Neurosci.* **30**, 596–602 (2007).
16. T. C. L. de Sampaio e Spohr, R. Martinez, E. F. Da Silva, V. M. Neto, F. C. A. Gomes, Neuro-glia interaction effects on GFAP gene: A novel role for transforming growth factor-β1. *Eur. J. Neurosci.* **16**, 2059–2069 (2002).
17. V. D. O. Sousa, L. Romão, V. M. Neto, F. C. A. Gomes, Glial fibrillary acidic protein gene promoter is differently modulated by transforming growth factor-β 1 in astrocytes from distinct brain regions. *Eur. J. Neurosci.* **19**, 1721–1730 (2004).
18. N. Morimura, T. Inoue, K.-I. Katayama, J. Aruga, Comparative analysis of structure, expression and PSD95-binding capacity of Lrfn, a novel family of neuronal transmembrane proteins. *Gene* **380**, 72–83 (2006).
19. C.-Y. Wang, K. Chang, R. S. Petralia, Y.-X. Wang, G. K. Seabold, R. J. Wenthold, A novel family of adhesion-like molecules that interacts with the NMDA receptor. *J. Neurosci.* **26**, 2174–2183 (2006).
20. J. Ko, S. Kim, H. S. Chung, K. Kim, K. Han, H. Kim, H. Jun, B.-K. Kaang, E. Kim, SALM synaptic cell adhesion-like molecules regulate the differentiation of excitatory synapses. *Neuron* **50**, 233–245 (2006).
21. L. Qin, X. Wu, M. L. Block, Y. Liu, G. R. Breese, J.-S. Hong, D. J. Knapp, F. T. Crews, Systemic LPS causes chronic neuroinflammation and progressive neurodegeneration. *Glia* **55**, 453–462 (2007).
22. S. Yao, Y. Zhu, G. Zhu, M. Augustine, L. Zheng, D. J. Goode, M. Broadwater, W. Ruff, S. Flies, H. Xu, D. Flies, L. Luo, S. Wang, L. Chen, B7-h2 is a costimulatory ligand for CD28 in human. *Immunity* **34**, 729–740 (2011).
23. Y. Zhu, S. Yao, B. P. Iliopoulou, X. Han, M. M. Augustine, H. Xu, R. T. Phennicie, S. J. Flies, M. Broadwater, W. Ruff, J. M. Taube, L. Zheng, L. Luo, G. Zhu, J. Chen, L. Chen, B7-H5 costimulates human T cells via CD28H. *Nat. Commun.* **4**, 2043 (2013).
24. J. A. Harrop, P. C. McDonnell, M. Brigham-Burke, S. D. Lyn, J. Minton, K. B. Tan, K. Dede, J. Spampanato, C. Silverman, P. Hensley, R. DiPrinzio, J. G. Emery, K. Deen, C. Eichman, M. Chabot-Fletcher, A. Truneh, P. R. Young, Herpesvirus entry mediator ligand (HVEM-L), a novel ligand for HVEM/TR2, stimulates proliferation of T cells and inhibits HT29 cell growth. *J. Biol. Chem.* **273**, 27548–27556 (1998).
25. J. R. Sedy, M. Gavrieli, K. G. Potter, M. A. Hurchla, R. C. Lindsley, K. Hildner, S. Scheu, K. Pfeffer, C. F. Ware, T. L. Murphy, K. M. Murphy, B and T lymphocyte attenuator regulates T cell activation through interaction with herpesvirus entry mediator. *Nat. Immunol.* **6**, 90–98 (2005).
26. G. Cai, A. Anumanthan, J. A. Brown, E. A. Greenfield, B. Zhu, G. J. Freeman, CD160 inhibits activation of human $CD4^+$ T cells through interaction with herpesvirus entry mediator. *Nat. Immunol.* **9**, 176–185 (2008).
27. K. M. Murphy, C. A. Nelson, J. R. Šedý, Balancing co-stimulation and inhibition with BTLA and HVEM. *Nat. Rev. Immunol.* **6**, 671–681 (2006).
28. C. F. Ware, Targeting the LIGHT-HVEM pathway. *Adv. Exp. Med. Biol.* **647**, 146–155 (2009).
29. G. Cai, G. J. Freeman, The CD160, BTLA, LIGHT/HVEM pathway: A bidirectional switch regulating T-cell activation. *Immunol. Rev.* **229**, 244–258 (2009).
30. T. C. Cheung, I. R. Humphreys, K. G. Potter, P. S. Norris, H. M. Shumway, B. R. Tran, G. Patterson, R. Jean-Jacques, M. Yoon, P. G. Spear, K. M. Murphy, N. S. Lurain, C. A. Benedict, C. F. Ware, Evolutionarily divergent herpesviruses modulate T cell activation by targeting the herpesvirus entry mediator cosignaling pathway. *Proc. Natl. Acad. Sci. U.S.A.* **102**, 13218–13223 (2005).
31. D. M. Compaan, L. C. Gonzalez, I. Tom, K. M. Loyet, D. Eaton, S. G. Hymowitz, Attenuating lymphocyte activity: The crystal structure of the BTLA-HVEM complex. *J. Biol. Chem.* **280**, 39553–39561 (2005).
32. Y. Wang, S. K. Subudhi, R. Anders, J. Lo, Y. Sun, S. Blink, Y. Wang, J. Wang, X. Liu, K. Mink, D. Degrandi, K. Pfeffer, Y.-X. Fu, The role of herpesvirus entry mediator as a negative regulator of T cell-mediated responses. *J. Clin. Invest.* **115**, 711–717 (2005).

33. Y. Sasaki, K. Ohsawa, H. Kanazawa, S. Kohsaka, Y. Imai, Iba1 is an actin-cross-linking protein in macrophages/microglia. *Biochem. Biophys. Res. Commun.* **286**, 292–297 (2001).
34. F. L. Heppner, M. Greter, D. Marino, J. Falsig, G. Raivich, N. Hövelmeyer, A. Waisman, T. Rülicke, M. Prinz, J. Priller, B. Becher, A. Aguzzi, Experimental autoimmune encephalomyelitis repressed by microglial paralysis. *Nat. Med.* **11**, 146–152 (2005).
35. K. Tamada, K. Shimozaki, A. I. Chapoval, G. Zhu, G. Sica, D. Flies, T. Boone, H. Hsu, Y.-X. Fu, S. Nagata, J. Ni, L. Chen, Modulation of T-cell-mediated immunity in tumor and graft-versus-host disease models through the LIGHT co-stimulatory pathway. *Nat. Med.* **6**, 283–289 (2000).
36. T. H. Watts, J. L. Gommerman, The LIGHT and DARC sides of herpesvirus entry mediator. *Proc. Natl. Acad. Sci. U.S.A.* **102**, 13365–13366 (2005).
37. R. Tao, L. Wang, K. M. Murphy, C. C. Fraser, W. W. Hancock, Regulatory T cell expression of herpesvirus entry mediator suppresses the function of B and T lymphocyte attenuator-positive effector T cells. *J. Immunol.* **180**, 6649–6655 (2008).
38. H. Dong, G. Zhu, K. Tamada, L. Chen, B7-H1, a third member of the B7 family, co-stimulates T-cell proliferation and interleukin-10 secretion. *Nat. Med.* **5**, 1365–1369 (1999).
39. I. M. Stromnes, J. M. Goverman, Active induction of experimental allergic encephalomyelitis. *Nat. Protoc.* **1**, 1810–1819 (2006).

Acknowledgments: We thank W. W. Hancock (University of Pennsylvania) for providing the HVEM$^{-/-}$ mice and B. Cadugan for editing the manuscript. **Funding:** This study was partially supported by U.S. NIH grants CA085721 and CA097085. **Author contributions:** Y.Z., S.Y., and L.C. designed the experiments, interpreted the data, and wrote the manuscript. Y.Z. performed most of the experiments and S.Y. made key contributions in identifying the receptor. M.M.A., J.W., J.S., and K.T. helped with the experimental design and data interpretation and performed/contributed to several experiments. H.X., M.B., W.R., L.L., and G.Z. contributed significantly in the execution of experiments. **Competing interests:** L.C. receives consulting fees from MedImmune and Pfizer, patent/licensing payments from Bristol-Myers Squibb, and sponsored research funding from Boehringer Ingelheim. The other authors declare that they have no competing financial interests. **Data and materials availability:** All data needed to evaluate the conclusions in the paper are present in the paper and/or the Supplementary Materials. Additional data related to this paper may be requested from the authors.

Submitted 19 May 2015
Accepted 8 March 2016
Published 8 April 2016
10.1126/sciadv.1500637

Citation: Y. Zhu, S. Yao, M. M. Augustine, H. Xu, J. Wang, J. Sun, M. Broadwater, W. Ruff, L. Luo, G. Zhu, K. Tamada, L. Chen, Neuron-specific SALM5 limits inflammation in the CNS via its interaction with HVEM. *Sci. Adv.* **2**, e1500637 (2016).